Spatial structure in diffusion-limited two-species annihilation

F. Leyvraz

Instituto de Física, Universidad Nacional Autónoma de México, Mexico City, Mexico

S. Redner

Center for Polymer Studies and Department of Physics, Boston University, Boston, Massachusetts 02215
(Received 17 April 1992)

We report on the spatial distribution of particles in the reaction $A + B \rightarrow 0$. For the spatial dimension $d \leq 4$, this process exhibits anomalously slow kinetics which stems from the formation of a mosaic of continuously growing domains which contain only one of the two species. We investigate the temporal evolution of the distribution of domain sizes, as well as the distribution of interparticle distances between closest-neighbor particles, both between the same and opposite species. Our results are considerably richer than might at first be expected. The average distance between closest-neighbor AB pairs scales differently than the corresponding distance between same-species pairs. The full distribution of AA separations is found to reflect the competing influences of these two length scales. Many of our observations can be accounted for in terms of simple scaling arguments. Rather surprisingly, many of our results are drastically altered if one of the species is immobile. The spatial distribution of the immobile reactant exhibits a self-similar character, leading to complex behavior for the moments of the interparticle distance distribution.

I. INTRODUCTION

A. Background

It has been recognized only fairly recently that the kinetics of the diffusion-limited reaction, $A + B \rightarrow 0$, does not conform to the predictions of mean-field theory [1–7]. This realization has stimulated considerable work in clarifying the mechanism for the breakdown of mean-field theory, and its implications on the kinetic behavior, both under transient [1–7] and steady-state conditions [8–11]. Furthermore, the reaction itself may be of interest in various "real world" contexts (such as annihilation of primordial monopoles in the early universe [2,4] and electron-hole recombination in irradiated semiconductors [12]).

The reaction process involves two species A and B which are originally distributed at random throughout space. They move by diffusion only and when two particles of opposite species approach within a fixed distance of each other (the reaction radius), they react irreversibly to form a third, inert species, which is then disregarded. A basic quantity that characterizes the kinetics is the time-dependent concentrations of the two species, $c_A(t)$ and $c_B(t)$, respectively. When the initial concentrations are unequal, the concentration of B's quickly decays to zero, whereas the concentration of A approaches a constant value. The focus of this work is the the case where the initial concentrations of A's and B's are initially equal, so that they remain equal throughout the reaction. [Due to their equality, we shall often refer to their common value as $c(t)$.] In this situation, $c(t)$ tends to zero relatively slowly, i.e., as a power law in time.

In a mean-field approximation, the time evolution of the concentrations is determined by writing down rate equations for $c_A(t)$ and $c_B(t)$. Under the assumptions of a purely bimolecular reaction mechanism and spatial homogeneity being maintained throughout the process, the rate equations are

$$\dot{c}_A = -kc_A c_B \, ,$$
$$\dot{c}_B = -kc_A c_B \, . \tag{1.1}$$

This gives, using the equality of the two concentrations,

$$c(t) = \frac{c(0)}{1 + kc(0)t} \sim (kt)^{-1} \, . \tag{1.2}$$

Thus the characteristic exponent of the long-time decay is -1, and the time scale is set by k.

However, it is well known that these results are incorrect for spatial dimension $d \leq 4$. In this case, domains containing only one of the two species form and diffusion is too slow a process to dissipate these domains. The existence of large-scale domains underlies the failure of the mean-field theory, since it is no longer true that the encounter probability between an A and a B particle is proportional to the product of their concentrations. We can establish the large time behavior of $c(t)$ by an argument that explicitly accounts for the local density fluctuations [2,3]. Within any finite volume Ω of linear dimension $\mathcal{L}$, the difference in the number of A and B particles can only change by diffusion, that is, when a particle leaves or enters Ω through the boundary. Then the difference $N_A - N_B$ will not be affected in its order of magnitude during a time $t_{\mathcal{L}}$ which is of the order of $\mathcal{L}^2/D$, where D

is the diffusion constant of the particles. However, at $t=0$, the difference is of the order to the square root of the initial particle number,

$$N_A - N_B \approx \pm\sqrt{c(0)}\mathcal{L}^{d/2} . \tag{1.3}$$

If we assume that species A is initially the local majority in Ω, then for $d \leq 4$, essentially no B particles will remain at time $t_{\mathcal{L}}$. Thus $N_A(t_{\mathcal{L}})$ is approximately equal to $\sqrt{c(0)}\mathcal{L}^{d/2}$, or, if one eliminates $\mathcal{L}$,

$$c(t) \approx N(t)/\mathcal{L}^d \sim \sqrt{c(0)}(Dt)^{-d/4} \quad (d \leq 4) . \tag{1.4}$$

This argument can be adapted to a variety of more general situations. In particular, it is easily seen that the above conclusion is not affected by the diffusion constants of the two species being different. Indeed, even in the extreme case where one species is immobile, the reasoning outlined above still applies. This approach is also valid, independent of the reaction rate k. If $k \ll 1$, however, a large crossover region of mean-field behavior will be observed, due to the fact that spatial heterogeneities which form at early stages of the reaction are transparent and therefore dissipate, due to the low reaction probability. For sufficiently large times, however, heterogeneities occur on a large enough length scale that they are opaque to the species in the local minority. Consequently, the fluctuation-dominated behavior of Eq. (1.4) ultimately results [3]. The basic argument can also be generalized to fractals, where one obtains that $c(t_{\mathcal{L}})$ is approximately given by $\sqrt{c(0)}\mathcal{L}^{-d_f/2}$, and $t_{\mathcal{L}}$ is equal to $\mathcal{L}^{d_w}$, leading to the time dependence $c(t) \sim t^{-d_s/4}$. Here, d_f is the fractal dimension, d_w is the dimension of a random walk on the fractal, and d_s is the spectral dimension. Although this last argument has been questioned [13], it appears that numerical results and independent analytical approaches are essentially in agreement with this prediction [14,15].

Thus we see that the kinetic behavior of the $A + B \rightarrow 0$ reaction is determined by the competition between A-rich and B-rich domains. In this paper, we will be interested in the geometrical properties of these domains and the distribution of reactants. We will address the following questions: what are the interparticle distances between closest-neighbor like and unlike species? How are they distributed? What is the distribution of domain sizes [16]? These questions turn out to have rather unexpected answers. We have previously reported [17] that the interparticle distances between like and unlike species grow with different powers of t for $d \leq 2$. More remarkably, these geometrical characteristics are rather sensitive to details of the reaction process itself. In particular, our previously reported scaling laws on distribution of interparticle distances and domain sizes are drastically modified in the case where one of the reactants is immobile.

The plan of this paper is as follows: We first describe the details of a lattice model for the reaction, and the particulars of our numerical simulations. In Sec. II we shall describe our results for the scaling behavior of interparticle distances, both between particles of the same and opposite species. In Sec. III we analyze the distribution of

domain sizes in one dimension by making analogies between the dynamics of domains walls in two-species annihilation and single-species annihilation. In Sec. IV we examine the density profile of domains, from which basic information about the distribution of distances between same-species particles can be inferred. In Sec. V we consider the distribution of interparticle distances, as well as the scaling of various moments of this distribution. Finally, we discuss the situation where the reaction occurs on a fractal substrate in Sec. VI. Throughout the paper, we will present analytical or scaling predictions wherever possible, and then bolster these by numerical simulation data. Further, we will generally consider separately the cases of equal mobilities and one species immobile, owing to the radically different behaviors in these two cases.

B. The model

Our simulation results are based on the following lattice model of the reaction process. We consider pointlike particles of two species A and B on a lattice. At each step of the simulation, we select a particle at random and attempt to move it to one of the nearest neighbors, again at random. If the target site is empty, the move is successful and the particle moves accordingly. If the target site is occupied by a particle of the other species, both the original and the target particle are removed with probability k. If there is a particle on the target site of the same species as the original particle, the move is rejected and the selected particle remains at its original position. This exclusion ensures that no multiple occupancy can occur, a feature which greatly simplifies the actual coding of this algorithm. After each move attempt, the time variable t is incremented by $1/N(t)$, where $N(t)$ is the current number of particles. This ensures that one unit of time corresponds approximately to having attempted to move each particle once, on average. In all cases, our simulations are performed with k set equal to one, as smaller values mask the effects we are interested in, and introduce an apparent mean-field behavior over a time scale of the order of $[D^d/k^4c(0)^2]^{1/(4-d)}$ [3]. For convenience, and also to provide an appropriate way to extrapolate exponent estimates, we perform measurements on the system at equal time intervals on a logarithmic scale. The results we report in one dimension are primarily based on the simulation of 900 realizations of the reaction for up to $1.5^{23} \simeq 11\,222$ time steps on a chain of 50 000 sites. For one specific application, we performed longer simulations, but with fewer realizations. In two dimensions, our results are based on averaging 50 realizations on a square lattice of linear dimension 500 for up to 50 000 time steps. Periodic boundary conditions are employed for all cases studied.

In three dimensions, it has been found that the model described above is not capable of reproducing, within numerically accessible times, the $t^{-3/4}$ decay of the density that is known to be correct in the long-time limit [7]. However, a rather minor modification of the aforementioned model can achieve this asymptotic behavior [18]. The procedure we followed is that when a particle is first selected, all of the neighboring sites are tested for occupancy by a particle of the opposite species. If opposite-

$$\underset{\text{AA}}{\ell} \qquad \underset{\text{AB}}{\ell}$$
$$\cdots\overline{A\ \overset{}{A}\ B\ B\ B\ A}\ \overline{A\ B\ A}\cdots$$
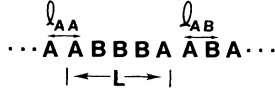$$|\longleftarrow L\longrightarrow|$$

FIG. 1. Definition of several basic interparticle distances that help characterize the spatial organization of reactants. Shown for the case of one dimension are the typical distance between closest-neighbor particles of the same species, l_{AA}, the closest-neighbor distance between unlike species, l_{AB} (or the length of the gap between domains), and the typical length of a domain, L.

species particles are found, the initially selected particle reacts with one of them (chosen at random) so that both are removed. Otherwise, a direction is chosen at random and the particle moves in this direction if the target site is empty. The overall effect of this procedure is to effectively increase the magnitude of the reaction rate and allow one to reach the asymptotic regime more rapidly. This modified model shows strong finite size effects, however, and must therefore be simulated on relatively large lattices. On a lattice with $\mathcal{L}=200$, the expected $t^{-3/4}$ decay was found to occur between $t=30$ and 1000, after which the finite size effects mentioned above lead to an exponential decay.

There are several natural ways to initialize the system. In one set of simulations, each site is occupied at random by an A, with probability $c_A(0)$, or a B, with probability $c_B(0)$. Since the actual number of particles in a finite system is typically unequal by an amount which is of order $\mathcal{L}^{d/2}$, spurious effects will occur at times of order $\mathcal{L}^2$, due to this existence of a true majority species. In one and two dimensions, these time are much larger than the range of our simulations. In three dimensions, however, this is not the case, and our simulations are affected by these resulting finite size effects. To avoid such problems, we put at random an exactly equal number of A and B particles, up to a prescribed lattice filling, which was usually taken to be unity. These two methods of initialization are found to give virtually identical results in the one- and two-dimensional cases.
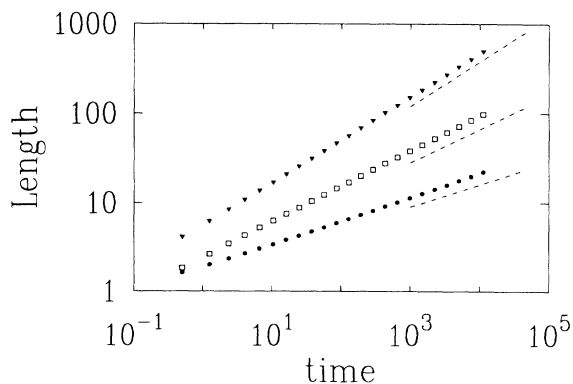

FIG. 2. Time dependence of the average distance between closest-neighbor particles of the same species, $\langle l_{AA}\rangle$ ($\bullet$); of opposite species, $\langle l_{AB}\rangle$ ($\square$); and the average domain length, $\langle L\rangle$ ($\blacktriangledown$). Shown are numerical results for a one-dimensional system when both species have the same mobility. The dashed lines of respective slopes $\frac{1}{4}$, $\frac{3}{8}$, and $\frac{1}{2}$ are a guide to the eye.

II. SCALING BEHAVIOR OF INTERPARTICLE DISTANCES

A. One dimension

To determine the behavior of the interparticle distances, we first introduce l_{AA} and l_{AB} as the distances between AA and AB closest-neighbor pairs, respectively (Fig. 1). Further, let c_{AB} be the concentration of AB closest-neighbor pairs. If we consider a time increment Δt of the order of l_{AB}^2/D, then there is sufficient time for essentially all AB closest-neighbor pairs to react, since one-dimensional random walks are compact. Consequently, the number of reactions occurring throughout the system, or the change in particle number, is of the order of $\mathcal{L}c_{AB}$. Dividing this change in number by the length of the system, one finds that the concentration changes according to [17]

$$\frac{\Delta c}{\Delta t} \approx -k\frac{c_{AB}}{l_{AB}^2/D}\ . \tag{2.1}$$

A straightforward generalization of this relation holds in two dimensions (with appropriate definitions of the various quantities involved, as outlined below), but not in higher dimensions, since the compactness of random walks is an essential ingredient in the derivation.

Since we independently know the behavior of $c(t)$, and hence of the left-hand side of Eq. (2.1), it is sufficient to have information on c_{AB} to determine the scaling behavior of l_{AB}. In one dimension, there is one AB pair per domain. Since domains have a typical size of $(Dt)^{1/2}$, one concludes that c_{AB} scales as $(Dt)^{-1/2}$, and hence

$$l_{AB}\sim[c(0)]^{-1/4}(Dt)^{3/8}\ . \tag{2.2}$$

There are several intriguing ramifications about this prediction. First, at least three lengths are needed to characterize the spatial distribution of the reactants (Fig. 2). From considerations of the kinetics alone, one deduces
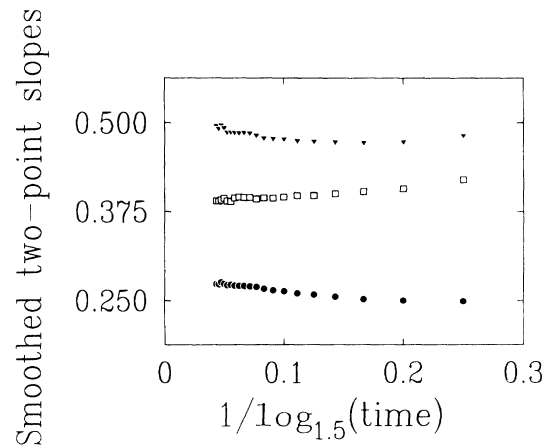

FIG. 3. Plots of the slopes of successive pairs of data points in Fig. 2 vs $1/\log_{1.5}t$. The symbols have the same correspondence as in Fig. 2. Averaging over consecutive pairs of data points has been performed to reduce nonsystematic fluctuations. The apparent exponent of $\langle l_{AA}\rangle$ is slowly increasing with time, and is slightly larger than $\frac{1}{4}$ at 11 222 time steps.

that the average domain size scales as $(Dt)^{1/2}$. Additionally, the typical interparticle spacing, which naively might be expected to coincide with the configuration average $\langle l_{AA} \rangle$, should scale as $[c(t)]^{-1}$, that is, as $t^{1/4}$. It is only through an explicit consideration of the spatial arrangement of the particles that one finds that $\langle l_{AB} \rangle$ scales differently than $\langle l_{AA} \rangle$. We can view this more rapid growth of $\langle l_{AB} \rangle$ as a manifestation of an effective "repulsion" between opposite-species particles. Nearby opposite-species pairs annihilate preferentially, leaving behind a population of opposite-species pairs which are further apart than the typical interparticle separation.

Another interesting point is the independence of $\langle l_{AB} \rangle$ on the reaction rate k. Notice that in Eq. (2.1) the rate constant k enters in a nontrivial way. Nevertheless, we have discarded it in writing Eq. (2.2), taking the rate constant to be of order unity. The theoretical motivation for this neglect is the fact that two particles separated by a distance $l \gg 1$ will collide not only once, but a large number (or order l) times in a time of order l^2. Thus, no matter how small k may be, the probability that a pair separated by a distance l reacts in a time l^2 is essentially one, a fact that we have also verified numerically.

The average separation between closest-neighbor same-species particles exhibits a rather puzzling behavior. As mentioned above, the time dependence of $\langle l_{AA} \rangle$ is characterized by an exponent which is close to, but measurably larger than the value of $\frac{1}{4}$ that one might naively expect (Fig. 3). Very roughly this larger exponent value stems from the nonhomogeneity of the local density. Since reactions are occurring only near the boundary of a domain, the local density must be smaller than in the central region of the domain. The range of this nonhomogeneity is controlled by the fact that the distance between two particles at the domain boundary scales as $t^{3/8}$. The relative sparseness in density near the domain interface permits the average distance between neighboring particles to be larger than the corresponding typical distance. In Sec. V we will estimate the influence of this local depletion when considering the density profile of a domain. In one dimension, the density inhomogeneity is found to give rise to an additional logarithmic factor in

the scaling behavior of $\langle l_{AA} \rangle$.

More remarkably, the interparticle distances exhibit a strong dependence on the mobility ratio of both species. In Fig. 4 we show simulation results for $\langle l_{AA} \rangle$ and $\langle l_{BB} \rangle$, when the B particles are immobile. In this case, note the very slow approach of the exponent for $\langle l_{BB} \rangle$ to its asymptotic value, whereas the time dependence of the exponent for $\langle l_{AA} \rangle$ is roughly the same as in the equal mobility case (Fig. 5). It is particularly disconcerting that the exponent for $\langle l_{BB} \rangle$ remains below $\frac{1}{4}$ over a large temporal range, since the asymptotic value of this exponent can be bounded from below by $\frac{1}{4}$. This bound can be established by considering an arbitrary one-dimensional system of identical particles whose concentration varies as $t^{-1/4}$. In this case, the average interparticle spacing l for a system of length $\mathcal{L}$ with periodic boundary conditions can be written as

$$l = \sum_{i=1}^{N} l_i / N = \mathcal{L}/N , \qquad (2.3)$$

where the summation runs over all nearest-neighbor pairs. Averaging this expression over all realizations immediately leads to

$$\langle l \rangle = \langle 1/c \rangle \geq 1/\langle c \rangle . \qquad (2.4)$$

Consequently, the exponent of $\langle l \rangle$ must be equal to, or larger than, $\frac{1}{4}$. The spatial organization effects of the $A + B \rightarrow 0$ reaction have a propensity to increase $\langle l \rangle$ with respect to $1/\langle c \rangle$ still further. As we shall discuss later, the smaller-than-expected value of the exponent for $\langle l_{BB} \rangle$ apparently stems from the self-similar domain structure of the B's, in which there is a power-law distribution of very-short-distance separations between neighboring B's.
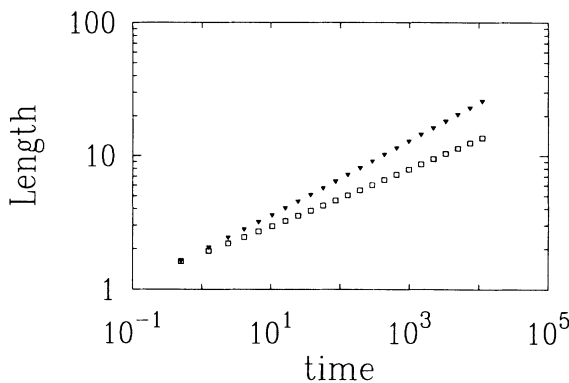

FIG. 4. Time dependence of the average spacing between closest-neighbor A's, $\langle l_{AA} \rangle$, and between closest-neighbor B's, $\langle l_{BB} \rangle$, ▼ and □, respectively, for a one-dimensional system when the B's are immobile.
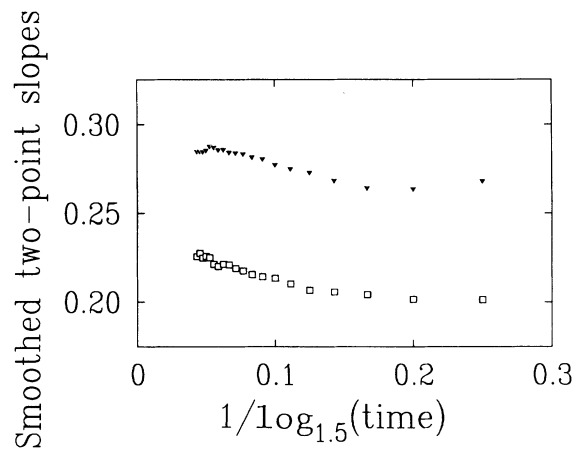

FIG. 5. Plots of the slopes of successive pairs of data points for $\langle l_{AA} \rangle$ and $\langle l_{BB} \rangle$, shown in Fig. 4, vs $1/\log_{1.5} t$. These results have been smoothed by averaging consecutive pairs of data points. The symbols have the same correspondence as in Fig. 4.

B. Higher dimensions

In greater than one dimension, the basic quantities and concepts we use to quantify the geometrical arrangement of the reactants are less easily defined than in one dimension. In particular, ambiguity arises in defining the closest neighbors of the opposite species for a given particle. If we were to consider only the closest two neighbors of a particle, as in one dimension, then there would be the risk of nearly always choosing neighbors of the same species, even for particles at the edge of a domain. However, Eq. (2.1) requires that we know which particles are most likely to react with a given particle. For this purpose, any reasonable definition of opposite species closest neighbors suffices. We have therefore used the following criterion: we define the m particles nearest to a particle as its neighbors, where we have taken m to be 6 in two dimensions and 10 in three dimensions (Fig. 6). While the choice of m is arbitrary, it is sufficiently large to almost always ensure that neighbors will be taken in all directions around the particle. This makes it overwhelmingly likely that at least one of the neighbors of a particle at the edge of a domain will be of the opposite species. We then define $\langle l_{AA} \rangle$ and $\langle l_{BB} \rangle$ as the average interparticle distances between same species, with the average taken over all AA or BB neighbor pairs. For $\langle l_{AB} \rangle$, we average over all AB and BA pairs. [It is an unavoidable feature of our definition that an A can be a neighbor of a B without the B being a neighbor of the A (Fig. 6).]

We now proceed to determine the time dependence of the interdomain distance gap in the same manner as in one dimension. For all $d \leq 2$, we still continue to apply Eq. (2.1), since it should hold whenever random walks are compact. Thus we again need to estimate c_{AB} in order to find the behavior of l_{AB}. To this end, we must determine how many particles are on the boundary of a domain. This determination requires two hypotheses: (i) The perimeter of a domain is smooth, that is, it has length $t^{(d-1)/2}$; and (ii) The particles in the perimeter zone are separated by a distance of the order of l_{AB}, irrespective of their species. This is a fairly natural assumption which we have also verified in the one-dimensional case. If this assumption were false, then a rather absurd geometry would result, in which boundary particles are neighbors both of like and unlike species, yet remain infinitely closer to like particles than to unlike particles.

From these assumptions, the number of reactants at the periphery of a domain scales as $(t^{1/2}/l_{AB})^{d-1}$. Hence the concentration of reactive pairs is this number divided by the volume of the domain $t^{d/2}$,
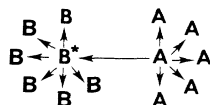
$$c_{AB}(t) \approx \frac{t^{-1/2}}{l_{AB}^{d-1}} . \qquad (2.5)$$

Following the logical consequences of Eqs. (2.1) and (2.5), we find

$$l_{AB} \propto t^{(d+2)/4(d+1)} , \qquad (2.6)$$

and, in turn, we deduce that

$$c_{AB}(t) \propto t^{-d(d+3)/4(d+1)} . \qquad (2.7)$$

In two dimensions, we have measured both $c_{AB}(t)$ and $l_{AB}(t)$ and find satisfactory agreement with the predicted values of the exponents. Our results give the value 0.83 for the exponent of c_{AB} and 0.33 for the exponent of l_{AB} (Fig. 7).

In three and higher dimensions, the situation is more subtle, as Eq. (2.1) is no longer valid. Now, it is relatively unlikely that two neighboring particles of the opposite species will react within a time of the order l_{AB}^2. Rather, they will do so with probability $l_{AB}^{-(d-2)}$, or in other
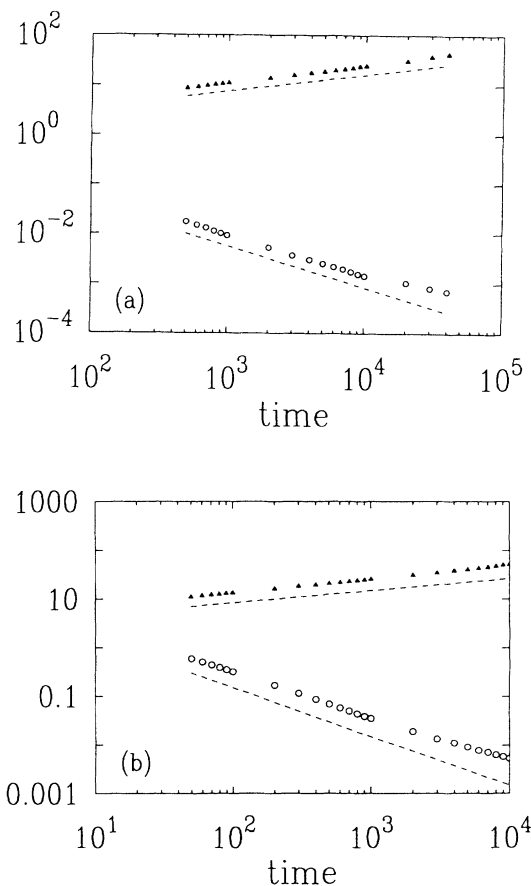

FIG. 7. Time dependence of the concentration of reactive pairs, $c_{AB}(t)$ (O), and the average distance between these pairs, $\langle l_{AB}(t) \rangle$ (▲), on (a) the square lattice, and (b) the simple cubic lattice. In (a) the dashed lines have slopes $-\frac{5}{6}$ and $\frac{1}{3}$, respectively, and in (b) the slopes of the dashed lines are -1 and $\frac{1}{4}$, respectively.

FIG. 6. Operational definition of the "neighbors" of an A particle in two dimensions. Note that the particle marked B^*, which is one of the neighbors of the A, does not include the initial A as one of its neighbors.

words, the characteristic time for two particles to meet, when confined to a region of linear dimension l_{AB}, scales as l_{AB}^d. Consequently, Eq. (2.1) must be modified to

$$\frac{\Delta c}{\Delta t} \approx -k\frac{c_{AB}}{l_{AB}^d} .$$

(2.8)

Using this relation, together with the additional assumption that the interfacial region between domains is smooth, i.e., the interfacial area scales as $t^{(d-1)/2}$, one obtains that, in three dimensions,

$$c_{AB} \approx t^{-1} ,$$
$$l_{AB} \approx t^{1/4} .$$

(2.9)

Thus the nontrivial scaling of interparticle distances disappears in three dimensions and above. Our numerical results, shown in Fig. 7, confirm the predictions of Eq. (2.9), and thus also length support to the hypothesis that the domain interface is a smooth object even when the spatial dimension is greater than 2.

III. DOMAIN SIZE DISTRIBUTION

A. The case of equal mobilities

In this section, we shall concentrate exclusively on the one-dimensional case. This is primarily motivated by simplicity, as it is difficult algorithmically to define a domain in higher dimensions. We could, of course, study the correlation functions between like and unlike species, but this only yields average properties of the distribution of reactants, aspects which are not the main goal of our study. Rather, we are interested in the distribution of domain sizes itself. To obtain information about this and related questions, one requires an easily computable way of partitioning the particles into A-rich and B-rich domains.

To gain a rough understanding of the distribution of domain sizes in the case of equal mobilities, it is convenient to focus on the dynamics of the domain walls, defined roughly as the point midway between two unlike neighboring particles. These domain walls annihilate upon contact, and we further postulate that they move diffusively (Fig. 8). Thus the dynamics of the walls (denoted by W) should coincide with that of the density of reactants in single-species annihilation, $W + W \to 0$, for which the kinetics has been solved exactly in one dimension [19–21]. The distribution of domain sizes in two-species annihilation then corresponds to the interparticle distance distribution in single-species annihilation. While this latter distribution is not known exactly, it is rigorously known that the distribution obeys single parameter scaling. Further, it has been proved that the scaling function decays exponentially for large values of the scaled separation x (defined as separation divided by
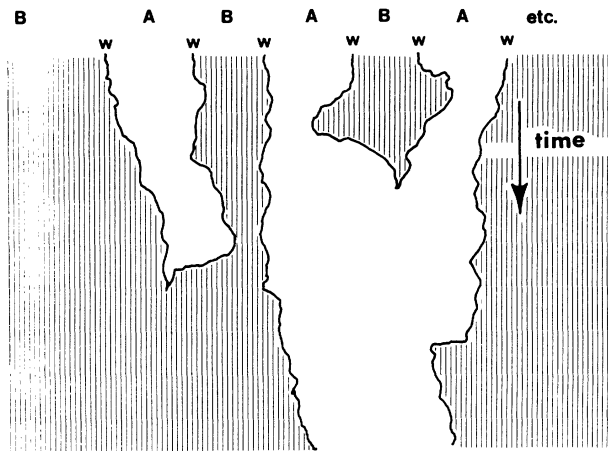

FIG. 8. Space-time representation of the $A + B \to C$ reaction in one dimension to illustrate the connection between the dynamics of domain walls (thin lines) and the single-species annihilation reaction, $W + W \to W$.

$t^{1/2}$), whereas the scaling function varies linearly in x for small x. For the sake of a self-contained discussion, we present simple heuristic arguments for these results.

The primary results about the interparticle distance distribution in single-species annihilation can be inferred in terms of known results for single-species fusion, $W + W \to W$ [22,23]. For this reaction, the scaled distribution of nearest-neighbor distances is exactly known to be

$$\Phi(x) = xe^{-x^2} .$$

(3.1)

This has similar properties to the interparticle distribution in single-species annihilation close to the origin, but falls off much faster as $x \to \infty$. We now construct an exact connection between these two processes by introducing the following general reaction scheme:

$$Y + Y \to Z ,$$
$$Y + Z \to Y ,$$
$$Z + Z \to Z .$$

(3.2)

In this composite process, properties of the Y's will be exactly as in the reaction $W + W \to 0$, whereas all properties that do not take the identity of the particle into account will coincide with that of the fusion reaction. Thus the interparticle distance between any two particles, irrespective of identity, will be distributed as in Eq. (3.1). In the mean-field approximation, the concentrations of Y and Z are asymptotically equal. Since the reaction mechanism itself does not inherently contain segregating tendencies, we assume there is no large-scale segregation of Y's and Z's. Then the probability of having an exceptionally nearby YY pair is simply half the corresponding probability for arbitrary pairs, so that a linear decay of the interparticle distribution in the fusion reaction for x close to zero is suggested. On the other hand, there is a natural way to obtain relatively distant YY pairs. This occurs

whenever an exceptionally long string of Z's separates two Y's. The probability of this event decays only exponentially in the number of intervening Z's, and hence in the distance. This is to be compared with the Gaussian decay for the probability of finding a large distance between two arbitrary particles.
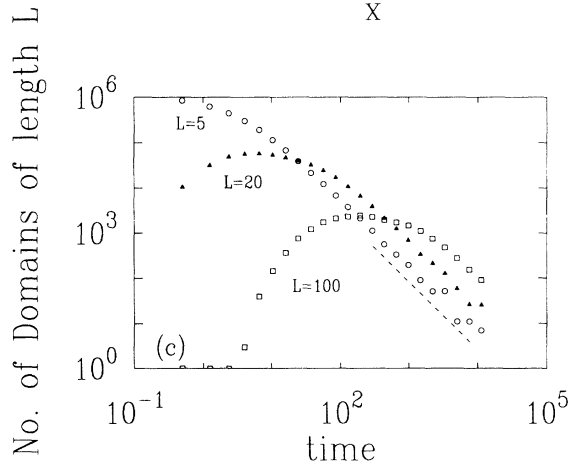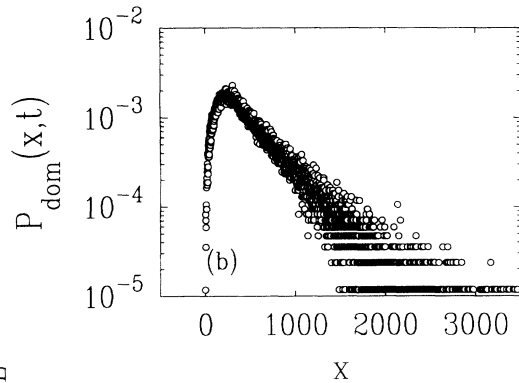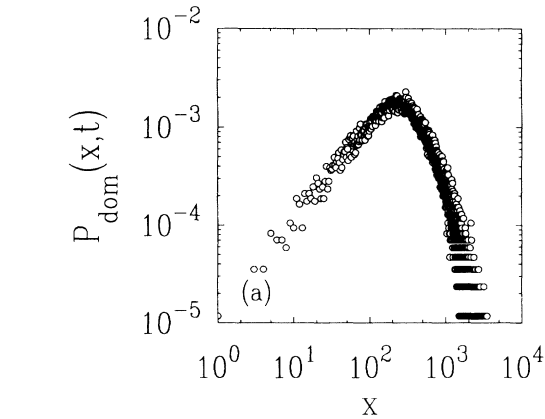
Based on these arguments, we are led to write the following scaling ansatz for $N(L,t)$, the number of domains of length L at time t;

$$N(L,t) \sim \frac{1}{t}\Phi(L/\sqrt{t}) \ , \tag{3.3}$$

where the scaling function $\Phi(x)$ has the following asymptotic behaviors (Fig. 9):

$$\Phi(x) \sim \begin{cases} x \ , & x \to 0 \\ e^{-Cx}, & x \to \infty \ . \end{cases} \tag{3.4}$$

Here the factor $1/t$ ensures that $\sum_L LN(L,t)$, which just gives the length of the system, is independent of time. This scaling form leads to a number of nontrivial consequences, such as the number of domains which are smaller than the typical size decaying as $t^{-3/2}$. This latter prediction is borne out by our simulations (Fig. 9).

B. The case of one immobile species

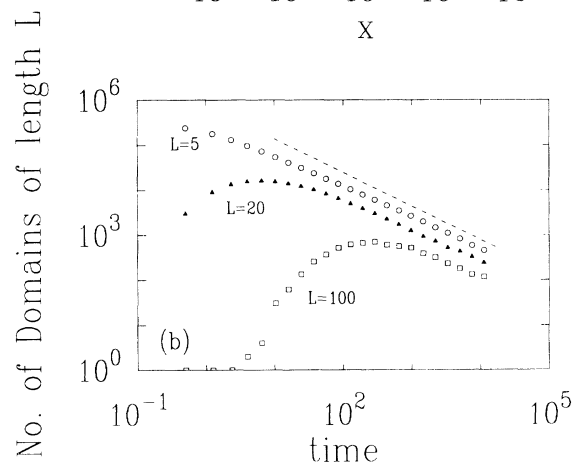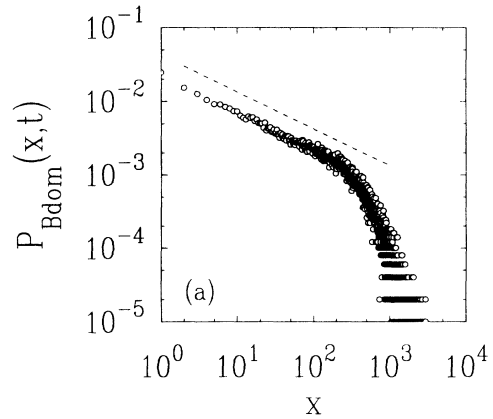If one of the two species, say B, is immobile, then the nature of the domain size distribution changes dramati-

FIG. 9. The (normalized) probability distribution of domain sizes, $P_{\text{dom}}(x,t)$, for the case of equal mobilities of A's and B's. Shown in the distribution at $t = 11\,222$ on a double logarithmic scale (a) to exhibit the linear behavior at small distances, and a semilogarithmic scale (b) to exhibit the large distance exponential tail. (c) Time evolution of the number of domains of fixed length L for several representative lengths. The dashed line has a slope $-\frac{3}{2}$.

FIG. 10. (a) The (normalized) distribution of domain sizes, $P_{B\,\text{dom}}(x,t)$, for the case of immobile B's. Shown is the distribution at $t = 11\,222$ on a double logarithmic scale to exhibit the power-law form at small distances. The dashed line has a slope of $-\frac{1}{2}$. (b) Time evolution of the number of domains of fixed length for several representative lengths. The dashed line has a slope $-\frac{3}{4}$.

cally. Numerical simulations in one dimension illustrate the basic new feature of a power-law tail for the small-size limit of the distribution (Fig. 10), in contrast to the peaked distribution in the equal mobility case. The observed value of the exponent is close to $-\frac{1}{2}$, a value which is suggestive of simple underlying mechanism. We offer the following explanation which arises from the dynamics of one-dimensional random walks.

Let us define the function $\rho(x)$ as the difference between the number of A and B particles in the interval $[0,x]$, where 0 is taken to be some fixed point in the system. Then a plot of $\rho(x)$ versus x is initially the graph of a typical one-dimensional random walk (Fig. 11). As time increases, this function becomes smoothed due to encounters between A and B particles as well as by the diffusion of A particles. Regions of positive values of $\rho(x)$ thus relax by diffusion and also spread to neighboring regions of negative $\rho(x)$. Up to time t, this spread is limited to length scales of the order of $\sqrt{t}$. Regions of negative $\rho(x)$, on the other hand, are affected by the annihilation process only, since the B's are immobile. Therefore as the system evolves, each region that is locally rich in A's initially, ultimately corresponds to a gap in a B domain which is of the order of the size of the original A-rich region. Up to time t, initial A domains of size $\leq \sqrt{t}$ will leave behind such a gap, while larger A domains will still survive. The gaps therefore have a size distribution identical to that of the positive regions in a one-dimensional random walk, except for a cutoff at a length of the order $\sqrt{t}$. The size distribution of such positive regions is the same as the probability that a one-dimensional random walk first returns to the origin [24], from which one infers that the distribution of the gaps of length x varies as $x^{-3/2}$, up to the cutoff (Fig. 11). Similarly, B domains are defined by the summation over BB

interparticle distances up to the cutoff that scales as $t^{1/2}$. Due to this integral relation between the distribution of interparticle separations and domains, we infer that the size distribution of the latter quantity varies as $x^{-1/2}$.

From this naive model, we can now infer the time dependence of the distribution of B domain sizes by applying a scaling argument in the spirit of the preceding section. Indeed, we expect the following scaling form for the number of B domains of length L:

$$N(L,t) \sim \frac{1}{t} \Phi(L/\sqrt{t}) \ , \tag{3.5}$$

with the arguments presented above indicating that

$$\Phi(x) \sim x^{-1/2} \quad (x \to 0) \ . \tag{3.6}$$

We also expect that $\Phi(x)$ vanishes exponentially for $x \to \infty$. It then immediately follows that the number of domains of a fixed size L vanishes as $t^{-3/4}$ as $t \to \infty$, as is borne out by the simulation data (Fig. 10).

IV. DENSITY PROFILES OF DOMAINS

A. General considerations

In this section, we study the distribution of particles inside a domain. Our primary focus is the one-dimensional case, due to the aforementioned difficulty of clearly defining what is meant by a domain in higher dimensions. Even in one dimension, however, there is an indeterminacy in the meaning of the density profile, and we have employed two natural definitions (Fig. 12). In both cases, we define the density as the probability of finding a particle at a fixed distance from the midpoint of a domain. Within a scaling formulation, it is convenient to rescale this distance by the domain size. This can be performed either using the typical domain size ("canonical" density profile) or the size of the domain to which the particle ac-
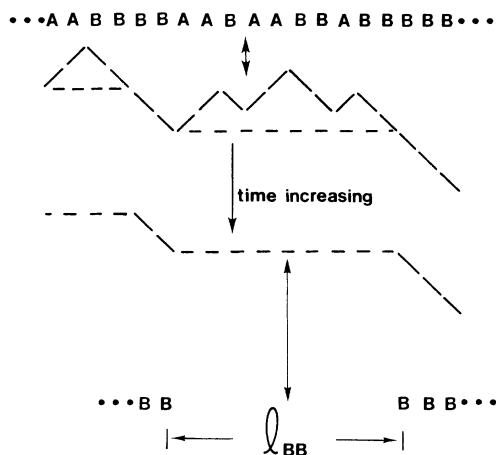

FIG. 11. Equivalence between an initial distribution of reactants and a one-dimensional random walk. The temporal evolution of this equivalent walk is also indicated: positive regions smooth out by diffusion, while negative regions are dissipated only by the diffusive invasion of positive regions. The gaps between the B's which ultimately remain coincide with the first passage of the equivalent random walk to the origin.
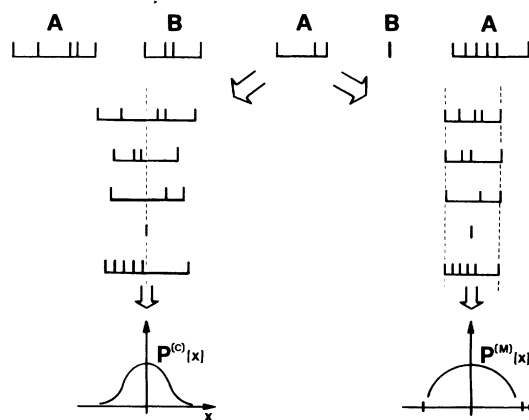

FIG. 12. Illustration of the construction for the "canonical" and "microcanonical" domain profiles from the original distribution of reactants. For the canonical profile, each domain is rescaled by the average length before their profiles are superposed. For the microcanonical profile, each domain is rescaled to a fixed length before superposition.

tually belongs ("microcanonical" density profile) as the rescaling factor. The qualitative appearance of the scaled profiles according to these two prescriptions is rather different, as shown in Figs. 13 and 14.

To obtain the canonical profile, we first superpose the densities of all domains with respect to their common centers, and then rescale the abscissa by the average domain size. The ordinate is therefore proportional to the density times the number of domains. Upon dividing by these factors, one obtains the normalized canonical density profile $P^{(C)}(x)$, the probability of finding a particle at a distance $xt^{1/2}$ from the center of the domain at time t. Note that the range of x is unbounded, in principle. For the microcanonical profile, each domain is first rescaled to the interval $[-1,1]$, which implies that the local density in the domain is now proportional to $t^{1/4}$. Upon superposing the density profiles of all domains and dividing by the product of the average concentration, the number of domains, and the average domain size, the normalized microcanonical distribution $P^{(M)}(x)$, is obtained.

FIG. 14. The microcanonical density profile for the case of immobile B's. The upper set of data are the profiles of the B's at $t = 194$ ($\circ$), $t = 1477$ ($\square$), and $t = 11\,222$ ($\triangle$). The lower set are the profiles of the A's at the same times. The profiles when both species are mobile are qualitatively identical to the data shown.
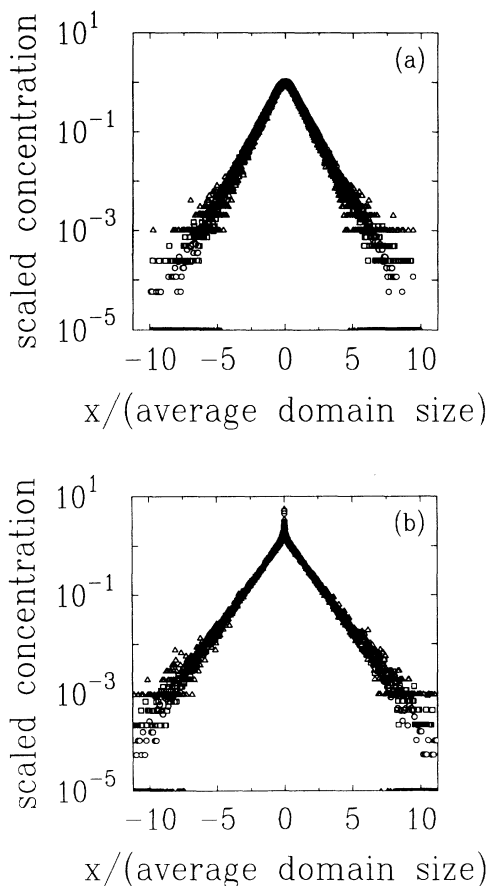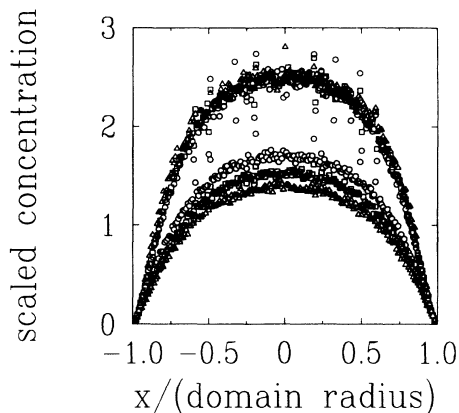

FIG. 13. Plots of the canonical density profile for the case of immobile B's. Shown are the scaled density profiles, summed over all realizations, of (a) the A's, and (b) the B's for $t = 194$ ($\circ$), $t = 1477$ ($\square$), and $t = 11\,222$ ($\triangle$). The former data are visibly indistinguishable from the canonical density profile when both species are mobile.

For the B's, this procedure leads to very accurate data collapse both for the equal mobility case and for the case of immobile B's (upper curve in Fig. 14). For the A's, excellent data collapse obtains for the equal mobility case; however, there is a small, but systematic deviation from data collapse for the case where the B's are immobile (lower set of curves). When these A profiles are rescaled by fixed powers of time, rather than by intrinsic quantities, excellent data collapse is found, however. Thus we attribute the evident lack of data collapse to the influence of nonasymptotic corrections in the various rescaling factors.

The behaviors of these two density profiles are simply related to each other. Namely, the contribution to the canonical density profile at scaled position x is equal to the microcanonical density profile at scaled position x/α, times the probability of finding a domain of scaled length α, summed over the possible values of α. This yields

$$P^{(C)}(x) = \int_x^\infty d\alpha \Phi(\alpha) P^{(M)}(x/\alpha) , \qquad (4.1)$$

where $\Phi(\alpha)$ is the scaling function for the probability of finding a domain of size $\alpha t^{1/2}$ introduced in the preceding section. Thus we expect that the large-distance tail of the canonical distribution should decay exponentially in x, as is clearly demonstrated by the simulation data (Fig. 13). An additional noteworthy feature of the canonical profile for immobile B's is the sharp peak near the origin. This stems from the square-root singularity in the size of B domains [Eq. (3.6)].

For the microcanonical profile, the profile resembles the half period of a sinusoid, independent of particle identity and the value of the diffusion coefficient. A crucial feature of this profile is the linear decay of the density in $1 - |x|$, as $|x| \to 1$. As we will discuss in more detail below, the feature controls the high-order moments of the distribution of distance between closest-neighbor same-species particles.

B. Domain wall dynamics

To account for a density profile which exhibits a linear decay at the periphery and a relatively constant density near the domain center, we consider an idealized model in which the A particles diffuse independently within a stochastically growing region defined by the two enclosing B domains. We represent the edge of these two enclosing domains by W (wall) particles, with the A and W particles reacting via

$$W + W \rightarrow 0 ,$$
$$W + A \rightarrow W ,$$
(4.2)

to provide a rough equivalent to two-species annihilation. The A's do not react with one another and their motion is characterized by a diffusion coefficient D_A. A priori there is no reason to postulate that domain walls have the same diffusion constant as the A's, or, for that matter, that they diffuse at all. However, we have already seen that considering the domain walls to be a system of annihilating random walks led to reliable results for the domain size distribution, so we shall assume that their motion is indeed diffusive, though with an unknown diffusion constant D_W.

For this simplified model, the problem of determining the density profile of A's within the domain now reduces to the distribution of a random walker between the two absorbing wall particles. This three-particle problem can be solved exactly if we neglect the possibility that one of the enclosing W particles might disappear in an encounter with another W before reacting with the A. With this approximation, the survival probability of such a walker is known [25,26] to vary asymptotically as $t^{-\pi/2\theta}$, with

$$\theta = \cos^{-1} \left[\frac{D_A}{D_A + D_W} \right] .$$
(4.3)

The existence of a power-law dependence for the survival probability of an A inside a domain is at least consistent with the $t^{-1/4}$ decay for the density. However, it must be noted that there is no value for the diffusion constant of the W particles which will give an exponent less than one for the time dependence of the decay of the A's. Thus the correct value of $\frac{1}{4}$ cannot be reached. This deficiency presumably stems from the neglect of reactions between W particles. Nevertheless, useful insights are gained from our mapping to a three-particle system; in particular, the density profile at long times is proportional to $\cos[\pi x / L(t)]$ for domain defined by $(-L(t)/2, L(t)/2)$. This sinusoidal variation provides a reasonable qualitative account of our numerical data for the microcanonical domain profile.

An even simpler approach that provides qualitatively similar results is to reduce the three-particle problem still further by assuming that the two absorbers deterministically recede from one another, with the distance separating them growing as $\sqrt{t}$. For this reduced problem, the density profile is given by the solution to the diffusion equation

$$\frac{\partial c(x,t)}{\partial t} = \frac{\partial^2 c(x,t)}{\partial x^2}$$
(4.4)

subject to the boundary conditions

$$c(-L(t)/2, t) = c(L(t)/2, t) = 0 ,$$
(4.5)

with $L(t) = C t^{1/2}$. This rate of growth is the maximum that can still be solved consistently within the adiabatic approximation [27]. This method leads to the density profile

$$c(x,t) \sim t^{-\lambda} \cos[\pi x / L(t)] ,$$
(4.6)

where λ is now an undetermined exponent that depends on the value of the amplitude C. Thus the form of the density profile is essentially the same for the cases where the W particles recede deterministically and where the W's move stochastically.

We have also investigated numerically the density profile for the situation of one immobile species. Rather remarkably, the microcanonical density profiles of the A's and the B's are virtually identical. There is also minimal visible difference between these two profiles and that of the equal mobility case. On the other hand, the canonical profile of the immobile species exhibits a relatively sharp cusp at the domain core (Fig. 13), a feature which undoubtedly stems from the power-law contribution of small BB separations, a singular behavior which is most likely to occur at the center of a domain. The coincidence between the microcanonical domain profiles for the equal mobility and immobile B cases is rather surprising, as the BB distances are distributed according to a power-law form at small distances. Evidently, the averaging involved in computing the density profile obscures this self-similar structure.

V. DISTRIBUTION OF INTERPARTICLE DISTANCES

A. The case of equal mobilities

From the above results about the domain profile it is possible to draw far-reaching conclusions for the distribution of interparticle distances. These inferences rely crucially on two basic features of the domain profile. First, we will exploit the fact that the microcanonical density profile of a domain vanishes linearly in the distance to the edge of the domain. We further assume that, apart from the variation in density on a length scale of order $t^{1/2}$, the A's are distributed locally at random. This is a reasonable assumption in view of the randomizing influence of diffusion.

Based on this latter assumption, we are led to write the probability of finding an AA separation of length l_{AA} as the Poisson form, $\rho e^{-\rho l_{AA}}$. Since ρ is of the order of $t^{-1/4}$, the typical values of l_{AA} will be of the order of $t^{1/4}$. To generalize to the situation where there are density variations on a scale of the domain size, we note that these variations are slowly varying, so that it is plausible to still write the local distribution of separations in a Poisson form. We therefore define the probability of encountering a closest-neighbor AA separation of length l_{AA} at time t at a scaled position z in the density profile as

$$P_{AA}(l_{AA}, z, t) = t^{-1/4} P^{(M)}(z)$$
$$\times \exp[-l_{AA} P^{(M)}(z) t^{-1/4}] , \qquad (5.1)$$

where $P^{(M)}(z)$ is the microcanonical density profile.

To obtain the average distribution of separations, irrespective of the position inside the domain, $P_{AA}(l_{AA})$, we integrate over the extent of the domain to yield

$$P_{AA}(l_{AA}, t) = \int_{-1+\epsilon}^{1-\epsilon} dz \, P^{(M)}(z)$$
$$\times \exp[-l_{AA} P_M(z) t^{-1/4}] . \qquad (5.2)$$

The range of the integral is over the populated region of the domain. Thus the cutoff ϵ (in scaled units) is determined by specifying that there is of the order of one particle between $z = -1$ and $-1+\epsilon$. In terms of the density profile, this condition reads [28]

$$\int_{-1}^{-1+\epsilon} P^{(M)}(z) dz \simeq t^{-1/4} . \qquad (5.3)$$

Since the shape of the density profile is linear near the end points, it immediately follows that $\epsilon \simeq t^{-1/8}$. Notice that this cutoff is merely the average gap length $\langle l_{AB} \rangle$ written in scaled units.

To obtain the interparticle distance distribution for $l_{AA} \gg t^{1/4}$, we use the saddle-point method to evaluate the integral in Eq. (5.2). Since $P^{(M)}(z)$ goes linearly to zero as $z \to \pm 1$, the end points will give the dominant contribution to the integral. From these considerations we find

$$P_{AA}(l_{AA}, t) \simeq l_{AA}^{-2} \epsilon^{-l_{AA} t^{-1/4} \epsilon} . \qquad (5.4)$$

Introducing a scaled variable x equal to $l_{AA} t^{-1/4}$, we may now write, for $x \gg 1$,

$$P_{AA}(x, t) \simeq x^{-2} \exp(-x t^{-1/8}) . \qquad (5.5)$$

From this form for the distribution of interparticle distances, we can now evaluate the scaling behavior of the corresponding moments,

$$\langle l_{AA}^n(t) \rangle = \int_0^\infty x^n P_{AA}(x, t) dx . \qquad (5.6)$$

By a direct calculation, we find, for the reduced moments $M_n(t) \equiv \langle l_{AA}^n(t) \rangle^{1/n}$,

$$M_n(t) \sim \begin{cases} t^{1/4} , & n < 1 \\ t^{1/4} \ln t , & n = 1 \\ t^{(3n-1)/8n} , & n > 1 . \end{cases} \qquad (5.7)$$

Most of these results are confirmed to a reasonable degree of accuracy by our numerical simulations (Fig. 15). A notable exception is the case $n = 1$, where the apparent exponent roughly extrapolates to a value close to 0.28. The actual numerical value of the exponent in the time

range of up to 10^4 time steps is consistent with what would be observed if $M_1(t)$ actually varied as $t^{1/4} \ln t$. However, the effective exponent is increasing with time, which does not accord with the hypothesized time dependence. Additionally, only part of the full scaling form of the distribution given in Eq. (5.5) seems to be accessible by simulations. The exponential large-distance decay can indeed be observed (Fig. 16), but the hypothesized x^{-2} decay takes place over too small a length range (from $t^{1/4}$ to $t^{3/8}$) to be measurable at the longest times that we simulated, 11 222 time steps.

We have also examined the distribution of AB distances (Fig. 17). As we expect, the distribution scales with $t^{3/8}$. With respect to the scaled distance x, the distribution of gap lengths goes linearly to zero as $x \to 0$, and decreases exponentially as $x \to \infty$. The former result is quite natural. Each particle which is part of an AB pair performs a random walk in which the other member of the pair acts as an absorber. Thus the limiting distribution ought to be similar to that of a random walker on
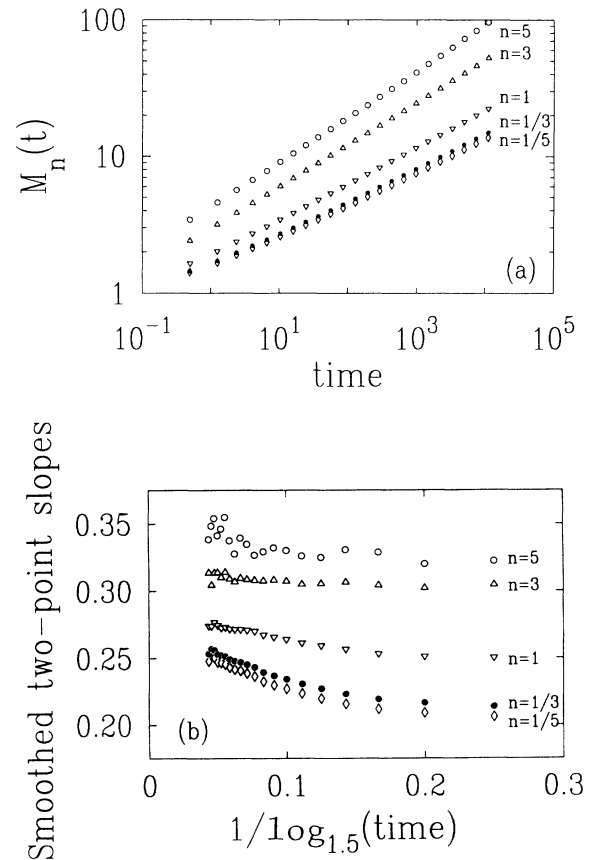

FIG. 15. (a) The reduced moments, $M_n(t) \equiv \langle l_{AA}^n(t) \rangle^{1/n}$, vs time on a double logarithmic scale for the case of equal mobilities of two species. Representative values of n are shown. (b) The behavior of the slopes between successive pairs of data points, smoothed by averaging consecutive data pairs and plotted vs $\log_{1.5} t$, to indicate the asymptotic value of the corresponding exponents for the time dependence of M_n.
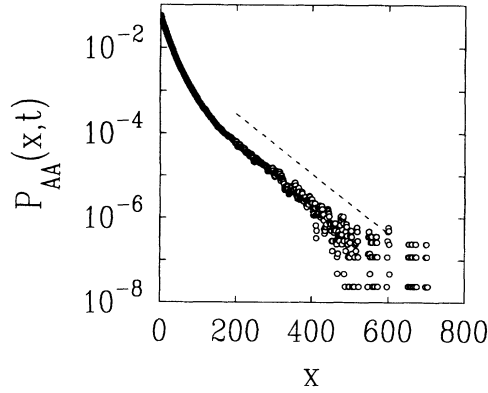
FIG. 16. The distribution of distances between closest neighbors of the same species, $P_{AA}(x,t)$, at $t=11\,222$ on a semilogarithmic scale to exhibit the large-distance exponential tail. The date are smoothed by averaging the distribution over five consecutive points. The slope of the best-fit straight line that fits the asymptotic decay (dashed and offset) varies as $t^{-3/8}$.

the half line, with an absorber at the origin. For this latter problem, the probability density decays linearly in x for $x \ll 1$, in accord with the small-distance behavior of the gap distribution. The origin for the exponential large-distance decay, as opposed to a Gaussian form, is not clear, however.
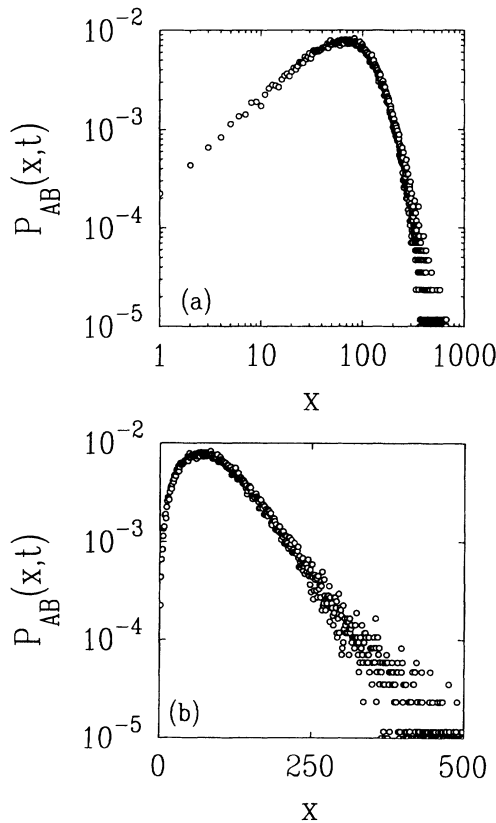

FIG. 17. The distribution of gap lengths between domains, $P_{AB}(x,t)$, at $t=11\,222$ on a double logarithmic scale (a) to exhibit the linear behavior at small distances, and a semilogarithmic scale (b) to exhibit the large-distance exponential tail.

B. The case of one immobile species

When one species is immobile, the situation is more complex, but also more interesting. Our numerical simulations indicate that the distribution of AA closest-neighbor distances has essentially the same form as in the case of equal mobilities for the two species. However, from the first-passage argument outlined in Sec. III, the probability of finding a BB closest-neighbor distance equal to x is proportional to $x^{-3/2}$ at small distances, a form that holds up to a characteristic distance which scales as $t^{1/2}$ (Fig. 18). For this form of the distribution, a simple calculation shows that the time dependence of the reduced moments of interparticle distances between the immobile species, $M_n(t) \equiv \langle l_{BB}^n(t) \rangle^{1/n}$, is

$$M_n(t) \sim \begin{cases} \text{const} , & n < \frac{1}{2} \\ \ln t , & n = \frac{1}{2} \\ t^{(2n-1)/4n} , & n > \frac{1}{2} . \end{cases} \quad (5.8)$$

Our numerical data for the reduced moments for positive integer n are in good agreement with the expectation of Eq. (5.8). Rather strikingly the reduced moments of order less than $\frac{1}{2}$ are predicted to have a finite limiting value as $t \to \infty$ (Fig. 19), a behavior which stems from the large number of exceptionally small BB distances. The fractional order moments do increase quite slowly with time in a manner that is consistent with their values reaching a finite asymptotic value [Figs. 19(a) and 19(c)]. The two-point slopes from successive pairs of data points all seem to extrapolate to zero in the long-time limit. However, for the range of times accessible in the simulation, it does not seem possible to identify unambiguously that the reduced moment of order $n=\frac{1}{2}$ is marginal in the sense of Eq. (5.8). Nevertheless the data are at least consistent with its predictions.

Owing to the broad distribution of sizes for the domains of immobile particles, it suggests that the relevant scaled distance between closest-neighbor BB pairs is their separation divided by the size of the domain to which the particular distance belongs, rather than di-
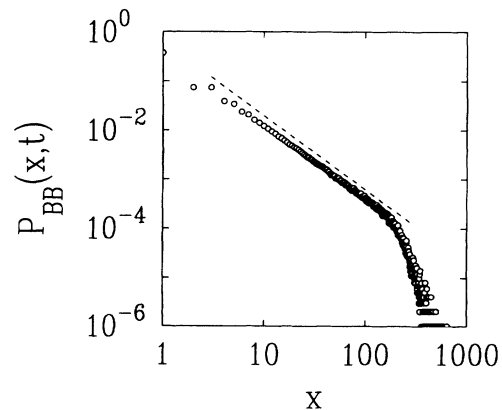

FIG. 18. The distribution of distances between closest-neighbor (immobile) B's, $P_{BB}(x,t)$, at $t=11\,222$. The dashed line has a slope $-\frac{3}{2}$.

viding by the average domain size. This scaling procedure is analogous to that used to obtain the microcanonical domain profile. Since the B's are immobile, there is a nonvanishing probability of finding a BB separation which is a finite fraction of the domain size. In contrast, diffusion tends to cut off the largest AA separa-
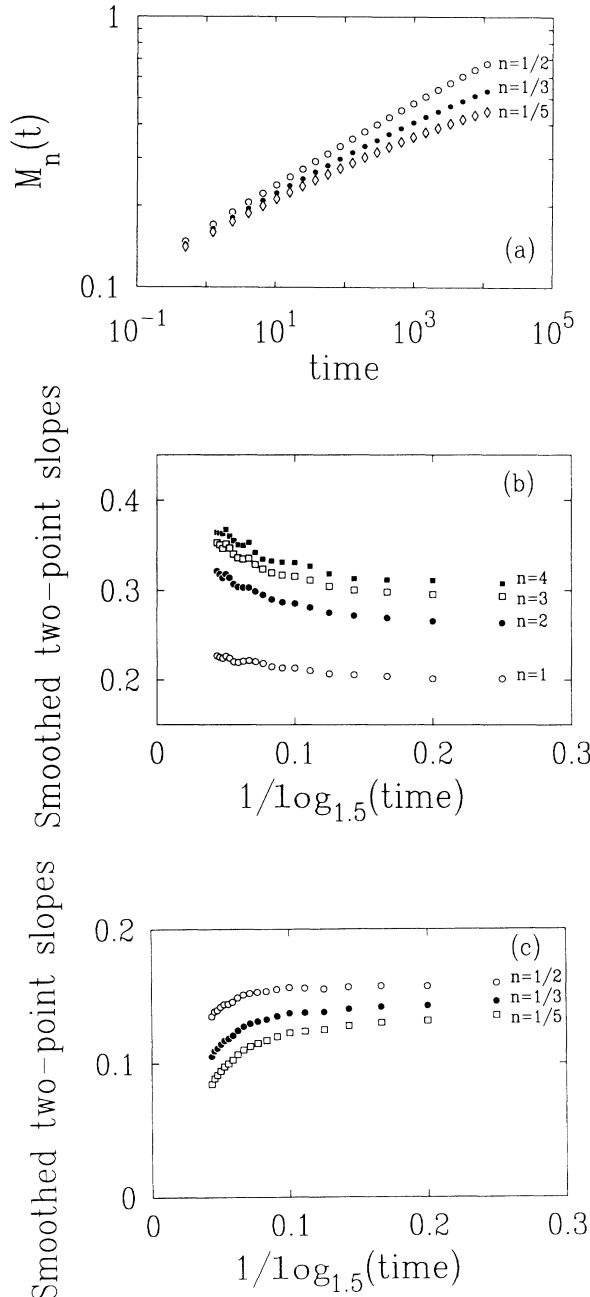

FIG. 19. Time dependence of the reduced moments $M_n(t) \equiv \langle l_{BB}^n(t) \rangle^{1/n}$ vs t on a double logarithmic scale for representative values of $0 < n < 1$ for the case of immobile B's. For positive integer values of n, the $M_n(t)$ all vary as power laws in time. In (b) and (c), we plot the smoothed slopes between successive pairs of data points for $M_n(t)$ to provide an estimate for the asymptotic value of the corresponding exponents for $M_n(t)$. Shown are these estimates for representative values of (b) $n > 1$, and (c) $0 < n < 1$.
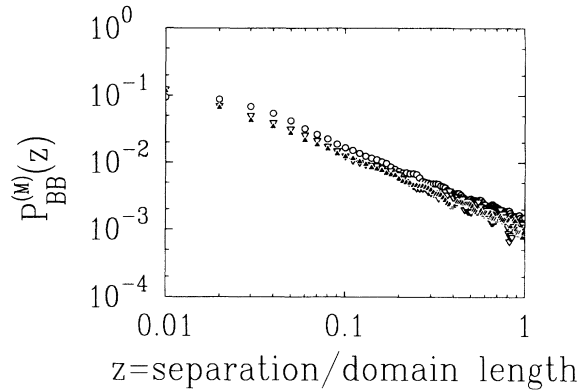

FIG. 20. The "microcanonical" distribution of BB separations for $t = 10^3$ (●), $t = 10^4$ (▲), and $t = 10^5$ (▽) on a double logarithmic scale.

tions at a scale which is of the order of $t^{3/8}$. This microcanonical approach yields a distribution of scaled BB separations which exhibits data collapse over a wide range of time scales (Fig. 20). This result provides additional evidence that the B's are fractally distributed within their domains.

C. Higher dimensions

In higher dimensions, we do not have numerical data for the density profile of a domain. Nevertheless, one can construct an approximate form for the density profile, using the same approach that was applied in one dimension. In greater than one dimension, we consider the density profile as being equivalent to the probability distribution of a particle diffusing within an absorbing ball whose radius is expanding as $\sqrt{t}$. The adiabatic approximation still applies for such a system and we therefore predict a density profile which decays linearly to zero in the radial coordinate near the extremity of the domain. From this fact, one can easily deduce scaling laws for the time dependence of the moments $\langle l_{AA}^n(t) \rangle$ which are amenable to numerical tests.

It is also worth noting that the linear decay in the density profile at the domain edge leads to an alternative and simple derivation of the fact that the AB distance scales as $t^{1/3}$ in two dimensions. Let us define T such that a shell of thickness T at the domain boundary contains of the order of $\sqrt{t}/T$ particles (Fig. 21). This provides a reasonable definition of the "outermost shell," since, on average, one particle will be contained in every area of linear dimension T. If the density profile decays linearly in the distance from the periphery of the domain, then the concentration in this outermost shell will vary as $t^{-1/2}(r/t^{1/2})$, where r is the distance from the edge of the domain. From this form, it follows that the entire outermost shell contains of the order of $T^2/\sqrt{t}$ particles. In order for this to coincide with $\sqrt{t}/T$, as required by the definition of T, it is necessary for T to scale as $t^{1/3}$, in agreement with the independent arguments given in Sec. II B, as well as with numerical results.

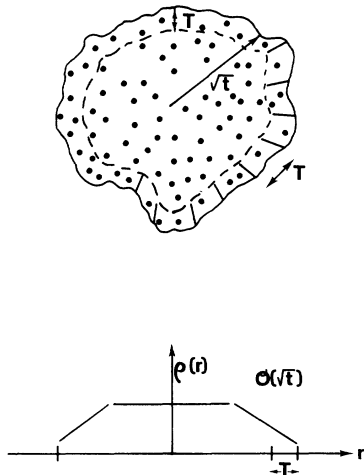Following exactly the same reasoning as in the one-

FIG. 21. Schematic illustration of the "outermost" shell of a domain. Also shown is the spatial variation of the density across the extent of the domain. The density stops varying at a distance of order $\sqrt{t}$ from the domain edge.

dimensional case, we now assume that the probability distribution of same-species interparticle distances l_{AA} in a region of local density ρ is given by the Poisson form $\sqrt{\rho/\pi}\,e^{-\rho l_{AA}^2}$. We now introduce the scaling variable $x = l_{AA}t^{-1/4}$, from which we obtain the following scaling expression for the number of AA pairs separated by a distance l_{AA}:

$$P_{AA}(l_{AA},t) = t^{-3/4}\Phi(x)\exp(-x^2 t^{-1/6}) , \tag{5.9}$$

$$\Phi(x) \sim x^{-3} \quad (x \gg 1) ,$$

where the normalization factor of $t^{-3/4}$ ensures that the quantity $\sum l_{AA}^2 N(l_{AA},t)$ remains time independent. The cutoff at x of the order of $t^{1/12}$ reflects the fact that there are no AA distances significantly larger than the typical AB distance, a criterion which has the same physical origin as in the one-dimensional case.

From this scaling form, one obtains the following scaling laws for the reduced moments $M_n(t) = \langle l_{AA}^n(t) \rangle^{1/n}$:

$$M_n(t) \sim \begin{cases} t^{1/4} , & n < 2 \\ t^{1/4}(\ln t)^{1/2} , & n = 2 \\ t^{(2n-1)/6n} , & n > 2 . \end{cases} \tag{5.10}$$

Our preliminary evidence suggests that the first two moments do not scale anomalously, but more extensive simulations are needed to adequately test the predictions of Eq. (5.10).

In summary, a considerable body of indirect evidence seems to indicate that the average density profile of a domain decays linearly in the distance to the edge of the domain in two dimensions. There is, however, no easy way to verify this assertion. An attempt to define a microcanonical density profile by superposing the profiles found on one-dimensional slices appears to give a decay of the density at the domain periphery which is nonlinear

in the distance to the edge of the domain. The reason for this discrepancy is as yet unresolved.

VI. THE REACTION ON A FRACTAL SUBSTRATE

As mentioned in the Introduction, the particle concentration should decay as $t^{-d_s/4}$ on a fractal substrate, where d_s is the spectral dimension [14,15]. There is an alternative theory which starts with specific hypotheses for the scaling of interparticle distances and uses these results to derive a different result for the decay of the density [13]. One of the underlying ingredients, however, is the claim that AA and AB distances scale in the same way, an assertion which has been found to be incorrect in the Euclidean case. Thus the conclusions of this approach should be viewed with caution.

In the following, we will take the view that $d_s/4$ is the correct decay exponent for a fractal. We shall then use Eq. (2.1) to infer a relation between the concentration of AB pairs and the scaling of the AB distance for the case where $d_s < 2$, i.e., for the situation where random walks are compact. For this purpose, we define the distance between two points as the number of steps in the shortest path connecting them (the so-called "chemical" distance). In terms of this chemical distance, we will require several additional characteristic exponents of fractals. These include the chemical dimension d_l, which describes the number of points $N(l)$ at a chemical distance l or less from the origin via the relation

$$N(l) \sim l^{d_l} , \tag{6.1}$$

the chemical dimension of a random walk d_l^w, which describes the typical time $t(l)$ required for a random walk to go a chemical distance l,

$$t(l) \sim l^{d_l^w} , \tag{6.2}$$

and the spectral dimension d_s, given by

$$d_s = \frac{2d_l}{d_l^w} . \tag{6.3}$$

This last exponent is also conveniently defined by the probability that a random walk is at the origin at time t, a quantity which decreases as $t^{-d_s/2}$. This implies that random walks on fractals with $d_s < 2$ are compact. For simplicity, and because these already form a vast majority of the fractals usually considered, we shall limit ourselves to this case.

We can now formulate our hypotheses concerning the nature of the domains and the interparticle distances.

(i) The domain boundaries are regular in the chemical distance, that is, they have chemical dimension $d_l - 1$. Here we see the importance of using the chemical distance: On a topologically one-dimensional object, such as the Koch curve, it is manifestly wrong to hypothesize that domain boundaries have dimension $d_f - 1$, where d_f is the fractal dimension. Rather the domain boundaries have dimension zero, which is what we obtain with our definition.

(ii) Same-species particles at the domain boundary are

separated by a distance of the order of l_{AB}. This basic assumption is the natural extension of the corresponding result on a Euclidean lattice.

From these assertions, we now obtain

$$c_{AB} \sim \frac{t^{-1/d_l^w}}{l_{AB}^{d_l-1}} . \tag{6.4}$$

Substituting this into Eq. (2.1), and employing $l_{AB}^{d_l^w}$ instead of l_{AB}^2 for the time needed for AB pairs to react, one obtains $l_{AB} \sim t^\zeta$, with

$$\zeta = \frac{d_l + 2d_l^w - 2}{2d_l^w(d_l + d_l^w - 1)} . \tag{6.5}$$

It should be emphasized that l_{AB} is a chemical distance. To obtain the corresponding scaling for the Euclidean distance, we use the connection $l = R^{d_f/d_l}$ between the chemical distance l and the Euclidean distance R between two points. Thus the Euclidean distance between closest-neighbor AB pairs involves the exponent $\zeta d_l/d_f$, with ζ given by Eq. (6.4).

In view of the peculiar nature of fractals and the attendant conceptual difficulties, the above results should be viewed as nothing more than tentative suggestions. Our predictions have some merits, however. They reduce to the correct results in the Euclidean case. Furthermore, they depend only on the connectivity of the fractal through the so-called "intrinsic" dimensions. The results are therefore unaffected by deformations, so that the Koch curve or the Peano curve are characterized by one-dimensional exponents. The principal weakness of our approach lies in the arbitrary nature of many of the hypotheses involved, specifically those concerning the geometry of the interface between two domains.

VII. CONCLUDING REMARKS

In diffusion-limited two-species annihilation, an initially homogeneous distribution of equal densities of A's and B's evolves into a mosaic of single-species domains which grow indefinitely with time. When both species are equally mobile, the concentration within the central region of the domains is roughly constant and is proportional to $t^{-d/4}$, while at the periphery the concentration vanishes linearly in the distance to the domain edge. This feature is responsible for the existence of a new length scale, l_{AB}, which is larger than the typical interparticle spacing and smaller than the typical domain size. This new length is of fundamental importance, as it determines the rate at which reactants are brought together. The depletion layer at the edge of the domain, and the attendant enhanced interparticle separations, is also responsible for the anomalous scaling of the moments of the distribution of distances between closest-neighbor same-species pairs. As a consequence, the reduced moments of the distribution of distances, $\langle l_{AA}^n(t) \rangle^{1/n}$, increase much more rapidly than the average separation between same-species particles, $\langle l_{AA}(t) \rangle$ when n is large.

When one of the species is immobile, the spatial organization of the reactants becomes considerably more rich. The domains of the immobile species are "eroded" by infiltration of the mobile species from the exterior. Thus vestiges of the initial distribution persist in the interior of the domains of immobile particles. In particular, this leads to a power-law tail for the number of small separations of the immobile particles. The reduced moments of the distribution of distances between closest-neighbor B's, $\langle l_{BB}^n(t) \rangle^{1/n}$, is now governed by this short-distance singularity, rather than by any large-distance enhancement. Thus we find very different time dependence for $\langle l_{AA}^n(t) \rangle^{1/n}$ and $\langle l_{BB}^n(t) \rangle^{1/n}$. In particular, the latter reduced moment approaches a constant as $t \to \infty$ for all $n < \frac{1}{2}$.

One ramification of our work is to two-species annihilation when the two components are initially separated, a problem which has recently been intensively studied [29–34]. For this system, considerable attention has been devoted to determining the spatial extent over which the reaction actually takes place. According to a mean-field treatment, the width of this reaction zone grows as t^ζ, with $\zeta = \frac{1}{6}$, a result which also appears to hold for simulations in two dimensions. However, in one dimension, a number of simulations give $\zeta \cong 0.3$ [33]. Following our treatment of the domain profile, the asymptotic concentration of order unity smoothly matches to a depletion layer of width $t^{1/2}$, in which the concentration vanishes linearly as the reaction zone is approached. These facts are sufficient to deduce that the separation between the closest AB pair grows as $t^{1/4}$. It should prove interesting to understand the relation between this separation and the width of the reaction zone.

In higher dimensions, we have a less than satisfactory understanding of the domain structure and the spatial organization of reactants. Thus far, we have not devised a good algorithm that unambiguously defines domains in greater than one dimension. We attempted to define a microcanonical density profile in two dimensions by superposing the profiles of one-dimensional slices. Unfortunately, this apparently natural definition gives a nonlinear decay of the density at the domain periphery, a feature which is at variance with our results about moments of interparticle spacings. Thus a better approach is needed to identify domains in two dimensions. Moreover, questions such as the distribution of domain sizes cannot even be meaningfully addressed in higher dimensions. The same is true for many aspects of the density profile within a domain. In three dimensions, our understanding of the domain structure is meager. Numerical evidence indicates that the anomalous behavior of the gap size no longer occurs, corresponding to no large-scale depletion in density at the domain edge. These results also suggest that the interface between domains is smooth, even for $d > 2$. All these results, however, still leave unresolved the question of how domains are organized spatially in higher dimensions.

[1] Ya. B. Zeldovich and A. A. Ovchinnikov, Chem. Phys. **28**, 215 (1978).

[2] D. Toussaint and F. Wilczek, J. Chem. Phys. **78**, 2642 (1983).

[3] K. Kang and S. Redner, Phys. Rev. Lett. **52**, 955 (1984); Phys. Rev. A **32**, 435 (1985).

[4] K. Lee and E. J. Weinberg, Nucl. Phys. B **246**, 354 (1984).

[5] G. Zumofen, A. Blumen, and J. Klafter, J. Chem. Phys. **82**, 3198 (1985).

[6] R. Kopelman, Science **241**, 1620 (1988).

[7] M. Bramson and J. L. Lebowitz, Phys. Rev. Lett. **61**, 2397 (1988); J. Stat. Phys. **65**, 941 (1991).

[8] L. W. Anacker and R. Kopelman, Phys. Rev. Lett. **58**, 289 (1987); J. Chem. Phys. **91**, 5555 (1987).

[9] K. Lindenberg, B. J. West, and R. Kopelman, Phys. Rev. Lett. **60**, 1777 (1988).

[10] D. ben-Avraham and C. R. Doering, Phys. Rev. A **37**, 5007 (1988).

[11] E. Clément, L. M. Sander, and R. Kopelman, Phys. Rev. A **39**, 6455 (1989).

[12] Z. Vardeny, P. O'Connor, S. Ray, and J. Tauc, Phys. Rev. Lett. **44**, 1267 (1980); see also *Laser Spectroscopy of Solids*, 2nd ed., edited by W. M. Yen and P. M. Selzer (Springer-Verlag, Berlin, 1986).

[13] W.-S. Sheu, K. Lindenberg, and R. Kopelman, Phys. Rev. A **42**, 2279 (1990); K. Lindenberg, W.-S. Sheu, and R. Kopelman, J. Stat. Phys. **65**, 1285 (1991).

[14] P. Meakin and H. E. Stanley, J. Phys. A **17**, L173 (1984).

[15] G. Zumofen, J. Klafter, and A. Blumen, Phys. Rev. A **43**, 7068 (1991); J. Stat. Phys. **65**, 1015 (1991).

[16] The importance of interparticle distributions in two-species annihilation was apparently first raised in P. Argyrakis and R. Kopelman, Phys. Rev. A **41**, 2121 (1990).

[17] F. Leyvraz and S. Redner, Phys. Rev. Lett. **66**, 2168 (1991); S. Redner and F. Leyvraz, J. Stat. Phys. **65**, 1043 (1991).

[18] F. Leyvraz, J. Phys. A **25**, 3205 (1992).

[19] M. Bramson and D. Griffeath, Z. Wahrsch. verw. Gebiete **53**, 183 (1980).

[20] D. C. Torney and H. M. McConnell, Proc. Soc. London, Ser. A **387**, 147 (1983).

[21] A. A. Lushnikov, Zh. Eksp. Teor. Fiz. **91**, 1376 (1986) [Sov. Phys. JETP **64**, 811 (1986)].

[22] J. L. Spouge, Phys. Rev. Lett. **60**, 873 (1988).

[23] C. R. Doering and D. ben-Avraham, Phys. Rev. A **38**, 3035 (1988); D. ben-Avraham, M. A. Burschka, and C. R. Doering, J. Stat. Phys. **60**, 695 (1990).

[24] See, e.g., W. Feller, *An Introduction to Probability Theory and its Applications* (Wiley, New York, 1968), Vol. 1, Chap. 3.

[25] D. ben-Avraham, J. Chem. Phys. **88**, 941 (1988).

[26] M. E. Fisher and M. P. Gelfand, J. Stat. Phys. **53**, 175 (1988).

[27] See, e.g., L. D. Landau and E. M. Lifshitz, *Quantum Mechanics* (Pergamon, New York, 1977).

[28] This approach for finding the "last" particle in a distribution was exploited for the case of a fixed trap by G. H. Weiss, S. Havlin, and R. Kopelman, Phys. Rev. A **39**, 466 (1989); S. Redner and D. ben-Avraham, J. Phys. A **23**, L1169 (1990); S. Havlin, H. Larralde, R. Kopelman, and G. H. Weiss, Physica A **169**, 337 (1990); H. Taitelbaum, R. Kopelman, G. H. Weiss, and S. Havlin, Phys. Rev. A **41**, 3116 (1990); H. Taitelbaum, *ibid.*, **43**, 6592 (1991).

[29] L. Gálfi and Z. Rácz, Phys. Rev. A **38**, 3151 (1988).

[30] Z. Jiang and C. Ebner, Phys. Rev. A **42**, 7483 (1990).

[31] H. Taitelbaum, S. Havlin, J. E. Kiefer, B. Trus, and G. H. Weiss, J. Stat. Phys. **65**, 873 (1991); H. Taitelbaum, Y.-E. Koo, S. Havlin, R. Kopelman, and G. H. Weiss, Phys. Rev. A **46**, 2151 (1992).

[32] S. Cornell, M. Droz, and B. Chopard, Phys. Rev. A **44**, 4826 (1991).

[33] M. Araujo, S. Havlin, H. Larralde, and H. E. Stanley, Phys. Rev. Lett. **68**, 1791 (1982); H. Larralde, M. Araujo, S. Havlin, and H. E. Stanley, Phys. Rev. A **46**, 855 (1992).

[34] E. Ben-Naim and S. Redner, J. Phys. A **25**, L575 (1992).